

## First experiments with lithium limiter on FTU

M.L. Apicella <sup>a,\*</sup>, G. Mazzitelli <sup>a</sup>, V. Pericoli Ridolfini <sup>a</sup>, V. Lazarev <sup>b</sup>,  
A. Alekseyev <sup>b</sup>, A. Vertkov <sup>c</sup>, R. Zagórski <sup>d</sup>, FTU Team <sup>a</sup>

<sup>a</sup> Associazione EURATOM-ENEA sulla Fusione, Centro Ricerche di Frascati, C.P. 65-00044 Frascati, Roma, Italy

<sup>b</sup> Troitsk Institute for Innovation and Fusion Research, Troitsk, Moscow Region, 142190, Russian Federation

<sup>c</sup> Federal State Unitary Enterprise "Red Star", 1A, Elektrolitnyi proezd, Moscow, 115230, Russian Federation

<sup>d</sup> Institute of Plasma Physics and Laser Microfusion, EURATOM Association, 01-497 Warsaw, Poland

### Abstract

A liquid lithium limiter (LLL) with capillary porous system has been tested for the first time on the high field medium size tokamak, FTU. Lithium acts as a first wall material in the liquid phase and as a conditioning technique by depositing a lithium film on the walls (lithization). Thermal loads exceeding  $5 \text{ MW/m}^2$  have been so far applied to the LLL surface during plasma discharges: no anomalous Li influx, like 'lithium bloom', occurs and no surface damage is observed, even after plasma disruptions. Radiation losses, plasma contamination and working gas recycling are reduced after Li coating of the wall as for boronization but with better results. A large electron temperature increase ( $\sim 50\%$ ) in the scrape-off layer occurs that is well reproduced by the simulation of 2D code TECXY. The Greenwald density limit is easily reached and even exceeded in the explored plasma current ranges ( $I_p = 0.50\text{--}0.9 \text{ MA}$ ).

© 2007 Elsevier B.V. All rights reserved.

PACS: 52.40.Hf; 52.55.Fa

Keywords: FTU; Limiter materials; Liquid lithium; Wall conditioning; Plasma facing components

### 1. Introduction

The interest on liquid lithium as plasma facing component for future fusion devices is driving a large effort in the recent years to gain experience on this attractive material. At present, extensive work on liquid lithium for fusion application is being carried out in the framework of the US Advanced Limiter-divertor Plasma-facing Systems

(ALPS) program that involves experimental and modelling activities [1]. On CDX-U, a small spherical tokamak, a liquid Li full toroidal limiter has been tested with promising results [1]. On the other hand the DIII-D experiments with a lithium sample exposed to the lower divertor put in evidence the critical role of  $J \times B$  forces on tearing the molten lithium off the container under high power exposure, possibly due to the specific conditions/geometry of the probe [1]. The problem of the mechanical stabilization of liquid lithium against  $J \times B$  forces has been faced and solved in the Russian Federation where a new concept for the lithium confinement

\* Corresponding author. Fax: +39 06 94005524.

E-mail addresses: [Apicella@frascati.enea.it](mailto:Apicella@frascati.enea.it) (M.L. Apicella), [Mazzitelli@frascati.enea.it](mailto:Mazzitelli@frascati.enea.it) (G. Mazzitelli).

based on a capillary porous system (CPS) in limiter configuration [2] has been developed and realized. This system could be easily adapted to supply Li by an external circuit for steady state reactor operations [3]. Very promising results have been obtained on T-11M tokamak, encouraging to extend the use of liquid lithium limiter on a more relevant fusion machine. An experimental program on this purpose started at the end of 2005 on FTU [4], an all metallic and carbon free medium size tokamak, with the aim to test for the first time in a high field machine a liquid lithium limiter (LLL) with CPS configuration. This paper describes the experimental results of the first experimental campaign in FTU on some important physical and technological issues such as: (1) the wall conditioning efficiency of lithium to reduce plasma contamination and recycling; (2) the lithium limiter capability to withstand high thermal loads from plasma interaction without surface damage. The paper is organized as follows: in Section 2, the CPS lithium limiter and its arrangement inside FTU chamber is illustrated followed by the description of the ‘lithization’ procedure that employs CPS LLL as a tool to deposit a lithium film on the chamber walls. In Section 3, the physical effects of lithization on plasma characteristics and in particular those produced in the scrape off layer (SOL), are described. Here a distinction will be made between the effects of Li coating on the walls without LLL inside the chamber and when it is inserted in the SOL. In Section 4 the thermal analysis of the lithium surface under plasma interactions are illustrated by comparing the experimental data and ANSYS code calculations. Finally the conclusions are drawn in Section 5.

## 2. CPS lithium limiter and lithization procedure

A prototype of liquid lithium limiter with CPS configuration has been developed for FTU [5]. It is composed by three similar units based on a mesh of capillaries of stainless steel 304, with pore radius 15  $\mu\text{m}$  and wires diameter 30  $\mu\text{m}$  that lead the liquid Li into contact with the main plasma from an underlying liquid reservoir. The dimensions of each module of the LLL, shown in Fig. 1, are, respectively, 100 mm and 34 mm in poloidal and toroidal direction. LLL can be heated up to 550  $^{\circ}\text{C}$  and is equipped with two Langmuir probes placed in the interspaces between units to monitor the electron density and temperature in the scrape off layer.



Fig. 1. Photograph of three units of lithium limiter installed on the support used for the LLL introduction inside FTU from the bottom vertical port. The dimensions of each unit of the LLL are: length = 100 mm, width = 34 mm. The two Langmuir probes are visible in the interspace between units.

Infrared detectors look at the three modules to monitor the lithium surface temperature during the plasma discharges [6]. The limiter is inserted from one vertical port at the bottom side of the machine and its radial position can be varied shot by shot. In this experimental campaign, the LLL was always located outside the last closed magnetic surface (LCMS) with the TZM (an alloy with 98% of Mo) toroidal limiter acting as main limiter. The toroidal limiter is in the high field side and its poloidal extension is  $\pm 35^{\circ}$  starting from the mid-plane. After plasma exposure lithium limiter can be extracted in a separated volume where an optical window permits to observe the Li surface. During the experimental campaign LLL has been used as lithium source for lithization during plasma discharge and as first wall material to test Li performance under progressively higher thermal loads in ohmic conditions. Two different operational conditions for lithium production have been checked: (a) physical sputtering of LLL in the scrape-off layer at the shadow of the LCMS during the discharge and (b) sputtering plus evaporation obtained by shifting the plasma towards the liquid lithium limiter, that it is in the same vertical position as in the case (a), to increase the thermal load and consequently the evaporation rate. In both cases lithium has been preliminarily heated up to 210  $^{\circ}\text{C}$  to be sure that Li was liquid before plasma exposure. The typical peak temperatures reached in case (a) and (b) were 350  $^{\circ}\text{C}$  and 450  $^{\circ}\text{C}$ , respectively. For an almost complete wall lithization, monitored by the temporal evolution of the Li III line intensity at 13.5 nm,

three shots (case a) at  $I_p = 0.5$  MA,  $n_e = 0.7 \times 10^{20} \text{ m}^{-3}$  with the LLL at a distance of about 2 cm from LCMS, are sufficient to obtain mainly lithium lines on the UV spectrum with O, Mo and Fe lines strongly reduced, respectively, by a factor 3.5, 1.8, 2.0. After lithization and LLL extracted from FTU, the Li III line intensity decreases shot by shot while the metallic lines increase again at a rate that is function of the input power.

Following a vent of the machine, traces of lithium have been found in the vacuum chamber with a nearly uniform toroidal distribution indicating that the lithium has been spread out by the plasma in a very efficient way. Unlike other tokamaks, FTU is a compact machine with narrow accesses, which do not permit an accurate investigation of the lithium film uniformity.

### 3. Physical effects on plasma characteristics

In this first experimental campaign the LLL has been tested in ohmic plasma discharges with  $B_T = 6$  T,  $I_p = 0.5$ – $0.9$  MA and average electron density  $n_e$  from 0.2 up to  $2.6 \times 10^{20} \text{ m}^{-3}$ . Plasma phenomenology after lithization, with LLL extracted from the vacuum chamber, is very similar to that observed after boronization [7] but with better results as shown in Fig. 2 for two discharges at  $I_p = 0.5$  MA,  $B_T = 6$  T after lithization (#28544) and after boronization (#28819). The fraction of the radiated power to the ohmic power is reduced by 50% and  $V_{\text{loop}}$  by  $\sim 10\%$  due to the lower  $Z_{\text{eff}}$  value. The electron temperature  $T_e$  also decreases, as a consequence of the smaller input power. For almost all the duration of the experimental campaign the effective ion charge values ( $Z_{\text{eff}}$ ) varied from 1.5 at low density ( $\bar{n}_e = 0.5 \times 10^{20} \text{ m}^{-3}$  to 1.0 at higher density  $\geq 1.0 \times 10^{20} \text{ m}^{-3}$ ). The most impressive result has been the strong capability of lithium to pump D particles allowing to extend the range of plasma operations to the lowest electron density never reached on FTU ( $1.5 \times 10^{19} \text{ m}^{-3}$ ). Only a small fraction of injected particles ( $N_g$ ) is found in the discharge as plasma particles ( $N_p$ ). The lowest value for the ratio  $N_p/N_g$  has been  $7.0 \times 10^{-3}$ , a factor 4 below that obtained after a fresh boronization, as reported in Ref. [7] which well describes the recycling characteristics of boronized and metallic walls. The saturation effects arising with a fresh boronization after high density pulses is not observed at all and the pre-programmed density is easily obtained. The operations

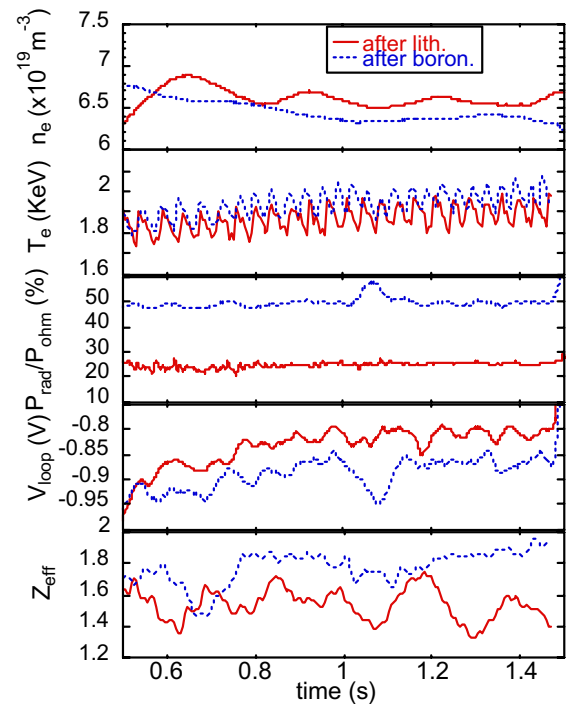


Fig. 2. Comparison between plasma parameters for two shots at  $I_p = 0.5$  MA,  $B_T = 6$  T after lithization and after boronization starting from the top with the average  $n_e$ ,  $T_e$ ,  $P_{\text{rad}}/P_{\text{ohm}}$ ,  $V_{\text{loop}}$ ,  $Z_{\text{eff}}$ .

near or beyond the Greenwald density limit are easily performed in the explored plasma current ranges ( $I_p = 0.50$ – $0.9$  MA). For  $I_p = 0.5$  MA,  $B_T = 6$  T, the density limit ( $\bar{n}_e = 2.7 \times 10^{20} \text{ m}^{-3}$ ) is 1.7 times higher than after a fresh boronization and a factor 1.4 higher than the corresponding Greenwald limit. In this case the electron density profile reaches a very high peaking factor  $n_{e0}/\langle n_e \rangle = 2.2$  [8]. Low particle recycling together with low radiation losses contribute to the increase of the density limit, which however does not increase with the plasma current as previously observed on FTU for plasma operations with Inconel or molybdenum poloidal limiters. The mechanisms that cause these peculiarities will be under specific investigation in the coming experimental campaigns.

Significant modifications of the scrape off layer, mainly of electron temperature, have been observed after lithization as a consequence of the strong pumping effect of lithium and the low core radiative losses that characterize these plasmas. The SOL plasma has been monitored along the poloidal circle by a set of a three reciprocating probes located at  $\theta \sim 0^\circ$  (external midplane), and  $\theta \sim -70^\circ$  (below

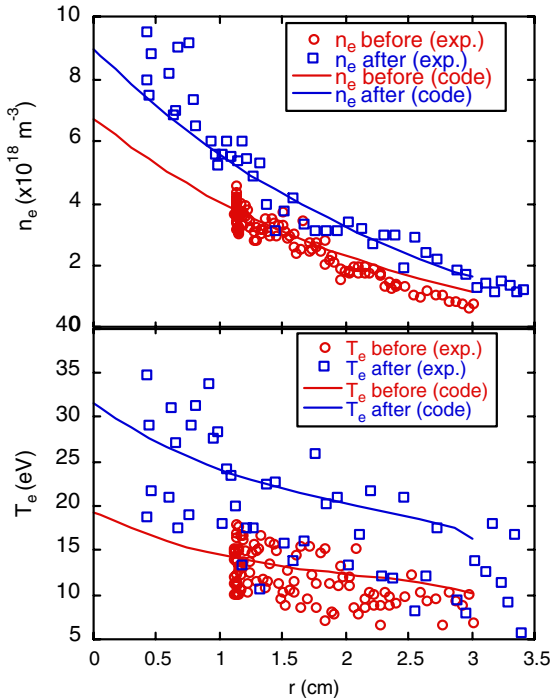


Fig. 3. Experimental (symbols) and code (lines) radial profiles of electron density (first frame) and electron temperature (second frame) in the SOL plotted against the minor radius after lithization (#28555) and for a clean metallic wall (#28482).

and  $\theta \sim 70^\circ$  (above) at  $\varphi = 120^\circ$  toroidally far from the LLL. In Fig. 3 the SOL electron density and temperature profiles are compared for two ohmic discharges having  $n_e = 6 \times 10^{19} \text{ m}^{-3}$ ,  $I_p = 0.75 \text{ MA}$  and  $B_T = 6 \text{ T}$  as main parameters, with  $Z_{\text{eff}} = 3.9$  (Mo plus a little amount of O) before lithization and  $Z_{\text{eff}} = 2.0$  (Li plus a little amount of Mo) after lithization. Despite the input power into the SOL is equal in both cases ( $P_{\text{in}} = 0.5 \text{ MW}$ ) and also the electron density profiles are very similar, the electron temperature values are strongly different, being higher by 50% for the shot after lithization. Such a large temperature variation has never been observed in any similar experimental situations on FTU.

In the same figure, we plot the results of simulations obtained with the 2D multifluid edge transport code TECXY [9], which is the extended version of the 2D EPIT code [10], already used on FTU to simulate plasma transport in the SOL. As input parameters for the 2D calculations we use the experimental parameters for the specific shots as well as the results of the global code named FTU-SELF that describes self-consistently the core (0D model) and the edge plasma (two-points model) of the FTU discharges [11].

It comes out from the simulations, that the SOL temperature in the shot before lithization is quite low because of the strong sink of electron energy due to the cooling rate characteristics of the Mo ions sputtered from the toroidal limiter surface. The radial diffusion and the recycling coefficient are not different from those typically used to simulate FTU data ( $D = 0.75 \text{ m}^2/\text{s}$ ,  $R = 0.75$ ) [7]. For the shot after lithization, instead, two important assumptions are needed to reproduce the experimental results: a strongly reduced recycling ( $R = 0.02$ ) related to the large pumping effect of lithium on the walls and a reduced contribution of Mo to the total radiation losses (the density of Mo at the LCMS must be set a factor three lower than before lithization). Assuming in the code Li as the only impurity in the SOL and a standard recycling coefficient  $R = 0.75$ , resulting  $T_e$  is much higher than in the experiment.

The same codes have been applied for shots with LLL inserted in the vacuum chamber. A full investigation of the SOL characteristics with lithium has been possible only in few plasma discharges when also the reciprocating Langmuir probes were inserted in the SOL. In all these cases the LLL was placed at the shadow of the main toroidal limiter at a distance of about 2 cm behind the LCMS. The following results are referred to a medium density shot ( $n_e = 1.0 \times 10^{20} \text{ m}^{-3}$ ) with  $I_p = 0.5 \text{ MA}$ , magnetic field  $B_T = 6 \text{ T}$  and  $Z_{\text{eff}} = 1.2$ . The analysis of the experimental data in the SOL shows that the profiles of plasma density were much steeper for the Langmuir probes magnetically connected with the LLL than for the other ones. As shown in Fig. 4 the e-folding length  $\lambda_n$ , is about twice shorter in a poloidal region extending poloidally  $10^\circ$  beyond the edge of the LLL magnetic shadow. However, no significant variation is observed for  $n_e$  and  $T_e$  values at the LCMS within the experimental errors. In addition to the measured values of  $n_e$  on the two Langmuir probes, which equip the LLL, stay in a ratio which well agrees with that deduced from the reconstructed magnetic topology. The code simulations confirm that the density profiles are much steeper in front of the LLL than in other poloidal positions and that the extension of the  $n_e$  and  $T_e$  perturbation is larger by about  $10^\circ$  than the poloidal extension of the LLL ( $\Delta\theta_{\text{LLL}} = 60^\circ$  and  $\theta_{\text{LLL}} = 270^\circ$ ). These results are due to the production of lithium atoms at the LLL and to the subsequent increase of the electron density due to the ionization of Li ions and to the local plasma cooling (that is



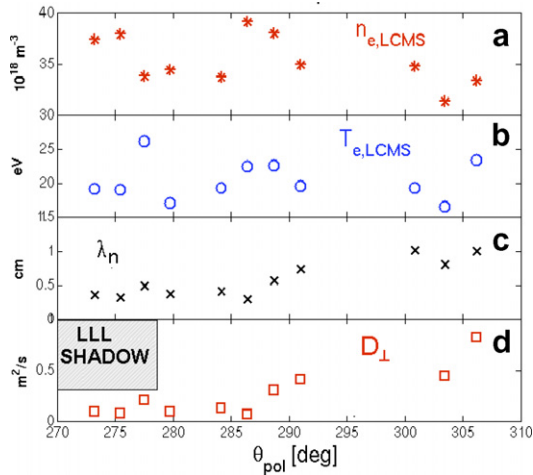


Fig. 4. From the top (a) and (b)  $n_e$ ,  $T_e$  at the LCMS, (c)  $\lambda_n$  and (d)  $D_{\perp}$  measured by Langmuir electrodes located in the bottom side of the machine plotted vs the poloidal angle.

not negligible because the plasma is not in coronal equilibrium). Since the LLL is poloidally close to the electron drift side of the toroidal limiter, the high density zone produced by interactions of plasma with LLL extends up to the main limiter. The contribution of D recycling is negligible.

#### 4. Thermal analysis

The behaviour of the lithium limiter as first wall material has been successfully tested for thermal loads exceeding  $5 \text{ MW/m}^2$  obtained by shifting the plasma towards the liquid lithium to increase the thermal load (case b). Thermal analysis of the heating dynamics has been carried out by using a 1D approximation for a semi-infinite body and by applying a more accurate model by means of ANSYS code [12]. In addition, these results have been compared with those obtained by the numerical simulations of TECXY code to assess the validity of the used methods. The surface temperature of the three LLL units has been measured by means of a special three-channel fiber-optic HgCdTe infrared detector developed for FTU to control fast variations of temperature from  $200^\circ$  to  $600^\circ\text{C}$  during plasma discharges. There is evidence, in some cases, that the Li surface temperature reaches a stationary phase, as it would occur in presence of a strong dissipative heat process [6]. In Fig. 5 the temporal evolution of the LLL surface temperature of the three limiter units, for the plasma discharge analyzed in Section 3, has been plotted together with the tem-

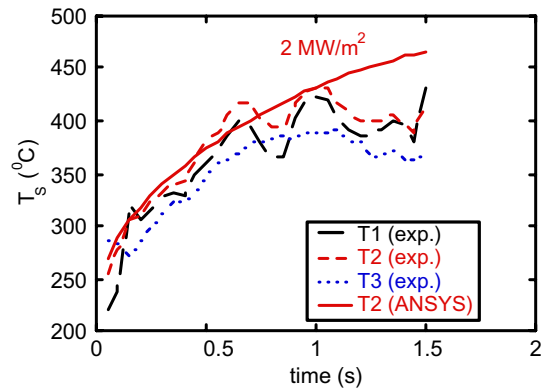


Fig. 5. Experimental temperature evolution for the three LLL units vs time. The temperature calculated by ANSYS code is also plotted for unit 2.

perature evolution as found from the calculations of ANSYS code for the unit #2 assuming a constant input thermal load of  $2.0 \text{ MW/m}^2$ . Surface temperature deviation from ANSYS calculation after about 1 s is related to a dissipative heat process not considered in the code as the Li radiation in front of the limiter surface. Calculations of TECXY code support this view; the total power to the LLL is estimated = 11 kW, which gives a power flux at LLL of the order of  $2.1 \text{ MW/m}^2$  on CPS surface well in agreement with ANSYS code.

The total  $D^+$  flux on the three Li limiter units is equal to  $\Gamma_{D^+} = 1.5 \times 10^{21} \text{ s}^{-1}$  as calculated from the average power fluxes  $q$  by the relation  $\Gamma_{D^+} = \Sigma_n(S_n q)/7T_e$  with  $T_e = 10 \text{ eV}$  (from Langmuir probes on LLL) and  $S_n$  equal to the effective area of the interaction surface ( $S_1 = 18 \text{ cm}^2$ ,  $S_2 = 16 \text{ cm}^2$ ,  $S_3 = 18 \text{ cm}^2$ ). Taking into account the evaporation rate and the  $D^+$  fluxes we conclude that Li flux is mainly produced by sputtering process ( $5.0 \times 10^{20}$  atoms) while evaporation contributes only for a small amount (about  $6.9 \times 10^{18}$  atoms).

The maximum increase of temperature on Li surface has not exceeded  $250^\circ\text{C}$  also in the case of stronger plasma interaction ( $>5 \text{ MW/m}^2$ ) due to the displacement of plasma position towards the lithium limiter surface.

No anomalous phenomena like ‘lithium bloom’ [13] occur during plasma discharges and no surface damage have been observed on the LLL after operations, also in the case of plasma disruption.

Nevertheless sometimes large spikes, as shown in Fig. 6, in the Li III intensity line have been observed without any increase in the LLL surface temperatures. These events are under investigation: unipolar

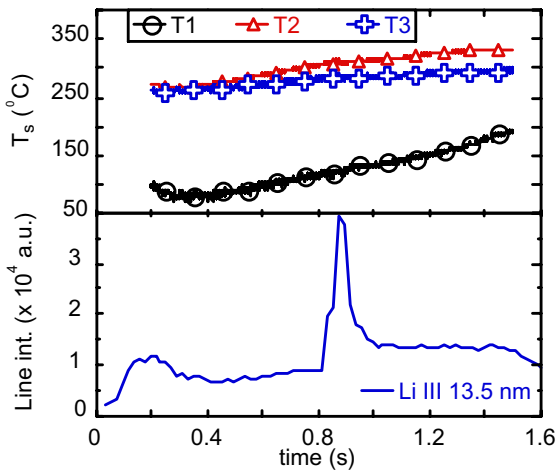


Fig. 6. Surface temperature evolution of the three LLL units and of Li III 13.5 nm line intensity.

arcs or droplets due to  $J \times B$  forces could be possible explanation. In other cases temperature peaks characterized by a sharp increase followed by a slower decay are detected by the infrared sensors with some correlation to plasma instabilities. After lithium experiments many droplets were found inside the vacuum chamber during the visual inspection. These droplets were only in two directions relative to the LLL surface: radially towards the high field magnetic side and perpendicularly towards the upper port. Instead they were completely absent in the toroidal direction. We believe that most of vertical droplets are generated as a consequence of plasma disruptions while those in the radial direction should be due to mechanical vibrations. Both these hypothesis are still under investigation.

## 5. Conclusions

A liquid lithium limiter has been successfully used for the lithization of the FTU vacuum chamber. Strong wall pumping capability and low values of  $Z_{\text{eff}}$  and of radiation losses have been obtained leading to improved plasma operations. The LLL has been also tested as plasma facing component for thermal loads exceeding  $5 \text{ MW/m}^2$  without any

surface damage or phenomena as ‘lithium bloom’. Events associated with strong increase in the VUV lithium line emissions were observed in non disruptive discharges whose origin will require more experimental investigations.

## Acknowledgements

Many thanks to L. Semeraro and his group for the mechanical project of the insertion mechanism of the LLL and the assistance during the installation on FTU, to the CODAS group for the remote temperature control and computer interface system, to the FTU operation group for the invaluable help during plasma operations and to R. Chirico, E. Di Ferdinando e M. Ciaffi for the technical support. One of the authors (R. Zagórski) acknowledges the support by the grant 3 T10B 00227 from the Polish Committee for Scientific Research (in years 2004–2007).

## References

- [1] J.N. Brooks et al., Fusion Sci. Technol. 47 (2005) 669.
- [2] V.A. Evtikhin, I.E. Lyublinski, et al., Fusion Eng. Des. 56&57 (2001) 363.
- [3] V.A. Evtikhin, I.E. Lyublinski, et al., Plasma Phys. Cont. Fusion. 44 (2002) 955.
- [4] F. De Marco, L. Pieroni, S. Santini, S.E. Segre, Nucl. Fusion 26 (1986) 1193.
- [5] M.L. Apicella, G. Mazzitelli, et al., Fusion Eng. Des. 75–79 (2005) 351.
- [6] A. Alekseyev et al., Proc. 33rd EPS Conference on Plasma Physics, Roma, Italy, June 19–23, 2006. On line at: <file:///Volumes/EPS2006/pdf/P1\_162.pdf>.
- [7] M.L. Apicella, G. Mazzitelli, et al., Nucl. Fusion 45 (2005) 685.
- [8] O. Tudisco et al., Proc. 33rd EPS Conference on Plasma Physics, Roma, Italy, June 19–23, 2006. On line at: <file:///Volumes/EPS2006/pdf/P5\_72.pdf>.
- [9] H. Gerhauser, R. Zagórski, et al., Nucl. Fusion 42 (2002) 805.
- [10] M. Leigheb, V. Pericoli, R. Zagórski, J. Nucl. Mater. 241–243 (1997) 914.
- [11] R. Zagórski, F. Romanelli, L. Pieroni, Nucl. Fusion 36 (7) (1996).
- [12] ANSYS users’ manual – SWANSON analysis systems, Inc.
- [13] V.B. Lazarev et al., in: 30th Conf. On Con. Fus. Pla. Phys., ECA2003, v.27A,P-3.162.